Contents lists available at Science-Gate

International Journal of Advanced and Applied Sciences

Journal homepage: http://www.science-gate.com/IJAAS.html

Transdermal drug delivery using low-frequency sonophoresis: COMSOL simulation of piezoelectric array transducers

Sehreen Moorat [1,*], Ahsan Ahmed Ursani [2], Aftab Memon [2], Nashrul Fazli Mohd Nasir [3], Majid Nour [4]

[1]Institite of Biomedical Engineering and Technology, Liaquat University of Medical Health and Sciences, Jamshoro, Pakistan
[2]Department of Biomedical Engineering, Telecommunication Engineering, Mehran University of Engineering and Technology, Jamshoro, Pakistan
[3]Faculty of Electronic Engineering Technology, Universiti Malaysia Perlis, Perlis, Malaysia
[4]Electrical and Computer Engineering Department, King Abdulaziz University, Jeddah, Saudi Arabia

ARTICLE INFO

Article history:
Received 17 January 2024
Received in revised form
22 May 2024
Accepted 27 May 2024

Keywords:
Sonophoresis
Low frequency
Transdermal drug delivery
COMSOL
Acoustic pressure
Mechanical index

ABSTRACT

This study explores the design and simulation of specialized sonophoretic transducers aimed at enhancing the transdermal delivery of large drugs. We examine different elements of the transducer's design, such as the choice of materials, its dimensions, and the matching of acoustic impedance. We selected PZT-4, from the lead zirconate titanate (PZT) group, as the main material due to its excellent piezoelectric features and durability. We also use polymer matrices to make the transducer less rigid. The simulation outcomes, using COMSOL Multiphysics, cover five different transducer array sizes (8x5, 10x6, 12x8, 14x9, and 16x10) within the frequency range of 20-40 kHz. We measure the acoustic pressure at a depth of 0.1 mm under the skin, which is key for successful drug delivery through the skin. Our results show how increasing the size of the array affects the transducer's efficiency. We confirm our simulation results by comparing them with a previously published ANSYS simulation and finding good alignment. This comparison adds reliability to our methods and outcomes. The study also proposes creating a small, wrist-mounted device for drug delivery that could be combined with drug patches, making it user-friendly. Moreover, we stress the need to follow Mechanical Index (MI) guidelines to avoid damaging the skin. Overall, our findings highlight the importance of the array size in the performance of the transducer and confirm the validity of our simulation approach, paving the way for innovative solutions in drug delivery that could have wide applications in healthcare.

1. Introduction

Transdermal drug delivery (TDD) stands at the forefront of pharmaceutical innovation, offering a revolutionary approach to drug administration by providing a non-invasive means of delivering therapeutic agents through the skin's epidermal layer (Yu et al., 2021). The epidermis, serving as the body's vigilant guardian against external threats like bacteria and harmful substances, presents an imposing barrier to drug penetration (Abe and Nishizawa, 2021). Within the epidermis, the stratum corneum (SC), the outermost layer, assumes the role of a major permeability barrier. While the SC is indispensable for overall skin health, it poses a formidable challenge for TDD systems. These systems must ingeniously find ways to temporarily and locally disrupt the SC, facilitating drug delivery without compromising the skin's integrity.

To overcome these formidable challenges, TDD systems employ active and passive methods for drug permeation. Passive methods effectively serve drugs with molecular weights below 500 Daltons (Krisnamurti et al., 2022). For drugs exceeding this threshold, active methods become essential. The repertoire of active methods includes techniques like iontophoresis, sonophoresis, electroporation, photomechanical waves, microneedling, and thermal ablation (Phatale et al., 2022).

Among active methods, low-frequency sonophoresis (LFS) has emerged as a focal point of interest in recent years. LFS harnesses ultrasonic waves within the frequency range of 20 kHz to 100 kHz to facilitate the movement of drug molecules

* Corresponding Author.
Email Address: sehreen.moorat@lumhs.edu.pk (S. Moorat)
https://doi.org/10.21833/ijaas.2024.06.007
Corresponding author's ORCID profile:
https://orcid.org/0000-0002-9646-9537

through the skin (Sá et al., 2013; Park et al., 2019). At the heart of this process are sonophoretic transducers, often constructed from piezoelectric materials, which play a pivotal role. These materials, characterized by their ability to generate electric charges under stress (the direct effect) and undergo mechanical deformation in response to an electric field (the converse effect), hold the key to successful drug delivery (Zhu et al., 2021). Sonophoresis has found applications in a diverse array of fields, further underscoring its significance and potential. Sonophoresis is effective in transdermally delivering genes like the stem cell factor, luciferase, and hepatocyte growth factor. Moreover, ultrasound treatment has been shown to raise the transdermal concentration of siRNA by sevenfold and ovalbumin by fifteenfold, indicating its potential to boost the efficacy of transdermal therapeutic delivery (Singh et al., 2022). Ma et al. (2020) used sonophoresis to enhance the transdermal delivery of cisplatin for treating cervical cancer. The findings suggest that sonophoresis effectively increases cisplatin's penetration in a cervical cancer xenograft tumor model (Ma et al., 2020). The use of sonophoresis for ocular drug administration has shown potential in increasing the permeability of the cornea to various drugs, including antibiotics, steroids, and beta-blockers (Lee and Rhee, 2022).

In dermatology, the effectiveness of sonophoresis in reducing sebum production is studied by Koznarska-Buczkowska et al. (2022). Their method employed an ultrasound device coupled with a cosmetic ampoule filled with green tea extract. During the treatment, the ampoule's contents were administered for a duration of 10 minutes. The use of sonophoresis significantly reduced sebum production, as the results indicated (Koznarska-Buczkowska et al., 2022). A stretchable electronic facial mask is designed using sonophoresis to enhance the effectiveness of drugs. The effectiveness of this SEFM in boosting the penetration of hyaluronic acid was verified through animal testing, and its ability to increase skin moisture by 20% was confirmed through experiments on human subjects (Li et al., 2022). Li et al. (2022) studied the synergic effect of sonophoresis and microneedles on enhancing the skin permeability for AZT. The results demonstrated that sonophoresis significantly decreased the lag time and greatly increased the drug's maximum flux and overall permeation. Using microneedles in combination with sonophoresis enhanced these outcomes even more, showing that the combined effect can lead to even higher levels of drug flux and total permeation (Li et al., 2022). A conformable ultrasound patch (cUSP) significantly enhances the transdermal delivery of niacinamide by using intermediate-frequency sonophoresis. This cUSP incorporated piezoelectric transducers within a soft elastomer, forming cavitation pockets for improved contact with the skin. In an in vitro porcine model, the cUSP achieved a 26.2-fold increase in niacinamide transport after just 10 minutes of ultrasound exposure (Yu et al., 2023).

In addition to sonophoresis, other active techniques employed for TDD also yield improved drug transport results. Cordery et al. (2019) reported that using iontophoresis can increase the rate of delivery of BUP and NTX through the skin as compared with passive TDD. Their research findings reveal that employing iontophoresis substantially increases the skin's permeability to drugs like BUP and NTX, significantly enhancing their transdermal transport over passive diffusion methods (Cordery et al., 2019). Another study explores the transdermal delivery of flurbiprofen for treating plantar heel pain using iontophoresis. It reveals that the drug's permeated amount increases proportionally. This highlights electromigration as the primary mechanism driving the iontophoretic flux of flurbiprofen (Cai et al., 2020). Recently, Kim et al. (2020) conducted a pioneering investigation into delivering recombinant coronavirus vaccines transdermally using microneedle technology to combat COVID-19. This approach facilitated the administration of SARS-CoV-2 S1 subunit vaccines, leading to strong antigen-specific antibody responses observable two weeks post-immunization (Kim et al., 2020). Sergio et al. employ pressure waves to temporarily disrupt the stratum corneum. This proves to be an effective method for enhancing the deposition of drug molecules into the skin. Also, offers a viable solution for the cutaneous delivery of drugs, particularly when a rapid onset of action is essential (del Río-Sancho et al., 2020). Vaidya and Shende (2020) studied the combined effect of using sonophoresis, followed by electroporation, and then applying a cold laser to enhance the penetration of methotrexate. Their findings suggest that sonophoresis significantly improves drug mobility and reduces pain, leading to better treatment outcomes for rheumatoid arthritis (Vaidya and Shende, 2020).

In this study, sonophoresis is selected due to its negligible adverse effects on the skin. However, designing a sonophoretic array transducer and choosing the right material is a crucial component. The choice of piezoelectric material and its design are fundamental to the efficacy of the transducer. Therefore, the choice of piezoelectric materials for sonophoretic transducers is a critical one, with a plethora of options, including ceramics like lead zirconate titanate, barium titanate, lithium niobate, and composites combining polymers and ceramics (Sekhar et al., 2023). Each material boasts unique characteristics, wielding a significant influence over transducer efficiency and effectiveness. Besides sonophoresis, piezoelectric elements are found in a wide array of applications like sensors and actuators, quartz watches, microphones and speakers, energy harvesting, etc.

Wang et al. (2021) developed piezoelectric wrist-worn energy harvester patches using finite element analysis. It worked on dual operational modes—impact and movement—to accommodate a range of human activities. Their study significantly enhanced the performance with maximum output achieved,

which is five times that of previous models (Wang et al., 2021). A similar simulation study on a piezoelectric array for energy harvesting was conducted by Kouritem et al. (2022). The results showed that altering the angle of the cantilever can increase the natural frequency, leading to higher output power (Kouritem et al., 2022). The experimental study conducted by Ji et al. (2021) highlights a piezoelectric micromachined ultrasonic transducer (PMUT) array's ability to detect deep defects in solids using a total-focus imaging algorithm. The findings suggest that PMUTs are not only adept at surface-level detection but also capable of deep solid imaging, not merely surface within hundreds of micrometers (Ji et al., 2021). A similar study was performed by Liu et al.(2021) using finite element analysis by Liu et al. (2021) Their work details the creation of a flexible 9-element PVDF PMUT array, utilizing bending mode with optimized resonance frequency and reduced crosstalk. The innovative adhesive bonding method allows for easy integration onto various surfaces, with demonstrated mechanical stability and flexibility in acoustic characterization. The potential for this technology extends to wearable and in vivo applications. COMSOL Multiphysics software has been extensively utilized in the modeling and development of piezoelectric transducers. The work by Bruno et al. (2018) evaluated the efficiency of a conventional bending actuator constructed using PZT ceramics and PMN-PT materials through COMSOL simulations. Furthermore, research by Zhang et al. (2018) focused on the design and creation of a medical phased array ultrasonic transducer, which demonstrated exceptional capabilities for biomedical imaging applications. Peng et al. (2019) introduced a groundbreaking ultrasound imaging system capable of tracking moving microbubbles for precision drug delivery and clinical purposes. In a similar way, Li and collaborators developed an acoustic liquid lens for piezoelectric transducers, enhancing the quality of imaging (Li et al., 2021).

Cavitation is one of the primary mechanisms underpinning sonophoresis. The sonophoretic stimulation of the skin triggers cavitation within the epidermis, causing structural alterations and heightened permeability (Zaid Alkilani et al., 2015). The presence of pre-existing gas bubbles within the lipid bilayer of the epidermis leads to cavity formation. Of particular importance is stable cavitation, which results in the cyclic expansion and contraction of these bubbles (Liu and Hsieh, 2009), effectively creating channels or pores within the epidermis. This process establishes a pathway for drugs to penetrate the skin, ultimately reaching their intended target (Mitra et al., 2014).

The primary focus of this paper is to pioneer the design and simulation of a sonophoretic transducer array meticulously optimized for the transdermal delivery of high-molecular-weight drugs. Our objective is to achieve the minimum peak acoustic pressure (AP) required for effective TDD, set at 0.23 MPa while maintaining an operating voltage as low as 1 volt. Furthermore, our long-term research vision extends beyond transducer design. We envision the development of a compact wrist-mounted TDD device seamlessly integrated with a drug patch, providing a user-friendly and convenient solution for patients in need of TDD. Wearable devices, despite their benefits, face a range of significant challenges, especially regarding their prolonged use. These challenges involve various aspects such as weight, battery life, user acceptance, and safety (Nahavandi et al., 2022). In this study, the piezoelectric transducer alone weighs ~66 g. Comparatively, the total weight of other wearable devices available in the market is approximately 120 g (Seneviratne et al., 2017). By prioritizing a compact design and incorporating the weight of existing wearable devices, the total weight of this device comes to ~187 g. To enhance battery longevity, we evaluate the transducer's efficiency by comparing different array sizes to find the setup that produces the highest AP at the lowest voltage (Grey and Hall, 2020). Utilizing a lower voltage helps prolong battery life, thereby minimizing the frequency of battery replacements. Meanwhile, available wrist-top devices employ Li-ion batteries with a capacity of 340 mAH. Consequently, even if the current is doubled from the transducer's maximum, the Li-ion battery can still comfortably support up to 34 hours of operation. User acceptance is pivotal to the success of wearable devices, with personalization, interface simplicity, and design being key factors (Ahmad et al., 2020). Therefore, this device is aimed to accommodate personal lifestyles by delivering the required amount of drugs along with monitoring other body parameters. The design is selected as inconspicuous, non-intrusive to daily life, comfortable for frequent wear, and maintains proximity to the body for precise sensing. Safety is an important issue when it comes to wearable devices. Therefore, the materials used are biocompatible to reduce the risk of allergic reactions or skin irritations (Lu et al., 2023). However, batteries should be designed to prevent overheating, which can lead to burns or even explosions.

The safety concerns associated with a sonophoretic transducer stem from the acoustic waves it generates. When these waves are passing through human tissue, they can cause tissue damage (Čáp et al., 2021). It happens due to thermal and non-thermal processes affecting biological systems (Han et al., 2023). The thermal effects are mainly caused by the temperature elevation on power, transducer aperture, tissue types, beam dimensions, and scanning mode. In contrast, non-thermal effects involve mechanical phenomena, notably cavitation, which is the production, oscillation, and collapse of gas-filled bubbles (Izadifar et al., 2017). The benefit-risk ratio of these effects can be measured by thermal index (TI) and mechanical index (MI). TI values aim to provide users with a rough indication of the probable maximum temperature increase during ultrasonic exposure under specific settings

(Tu et al., 2021). The method for determining the TI depends on the tissue model and exposure conditions. For example, TIS is used for soft tissue in the sound path (like abdominal scanning), TIB is for bone near the focus of the beam (such as in 2nd and 3rd trimester scanning), and TIC is for bone at the surface (such as in pediatric or adult transcranial scanning) (Fatahi Asl et al., 2021). Generally, thermal indices represent steady-state estimates calculated from the acoustic output power needed to heat a target tissue. This calculation involves the ratio of the attenuated acoustic power at a specified point (P) to the attenuated acoustic power required to increase the temperature at that point by 1°C (Pdeg), utilizing a homogeneous tissue model with an attenuation of 0.3 dB cm-1 MHz-1 (Martin, 2010).

$$\mathrm{TI} = \frac{\mathrm{P}}{\mathrm{P_{deg}}} \quad (1)$$

Consequently, the TI is intentionally defined to be unitless and is capped at a maximum value of 6, ensuring a standardized approach to assessing potential thermal risks associated with ultrasonic exposure (Quarato et al., 2023). For the non-thermal effects, the excessive use of APs in sonophoresis carries the risk of inertial cavitation, which can cause irreversible damage to the skin surface. To mitigate this risk, we adhere to a metric known as the MI. The MI accounts for the fact that a given AP at lower frequencies exerts a more pronounced effect on biological tissues compared to the same pressure at higher frequencies (Sekhar et al., 2023). It is mathematically defined as (Duncan et al., 2023):

$$MI = AP\ (MPa)/\sqrt{f}(MHz) \quad (2)$$

where, AP represents the peak acoustic pressure, and f is the operating frequency (Seah and Teo, 2018; Moghaddam et al., 2017). The Food and Drug Administration (FDA) recommends an upper limit of 1.9 for the MI to ensure the safety of sonophoretic treatments (Şen et al., 2015).

Additional safety considerations linked to ultrasound transducers are direct contact hazards, chemical effects, excessive acoustic output, lack of proper training, and device malfunction. Regulatory bodies and international standards provide safety guidelines, ensuring clinical ultrasound devices minimize operator and patient risks (Hsieh et al., 2022). Healthcare providers mitigate these concerns by using proper settings, undergoing training, and maintaining equipment to adhere to safety parameters (Moyano et al., 2022). This multifaceted strategy is imperative to minimize risks and ensure patient safety during ultrasound treatments. Regulatory bodies such as the International Electrotechnical Commission (IEC) and the U.S. Food and Drug Administration (FDA) have established stringent standards to limit the maximum surface temperatures of ultrasound transducers and specify maximum allowable acoustic output levels (Kim et al., 2021). These measures aim to prevent excessive heating and potential tissue damage during ultrasound examinations. Equipment manufacturers contribute by incorporating cooling mechanisms and real-time acoustic power adjustment algorithms to minimize transducer self-heating and ensure uniform energy distribution (Quarato et al., 2023; Geoghegan et al., 2022). Additionally, thorough training protocols for operators emphasize the importance of adhering to safety guidelines, such as proper transducer handling and monitoring patient feedback during procedures. Patient education regarding the ultrasound process enhances safety by fostering a communicative environment where patients are encouraged to report discomfort (Conlon et al., 2022).

2. System description

The performance efficiency of piezoelectric transducers is contingent upon several critical factors, including material selection, transducer dimensions, and the precise matching of acoustic impedances. Fig. 1a offers an illustration of a piezoelectric composite comprising an active layer and a polymer matrix. For our research, we have chosen PZT-4, an active piezoelectric transduction material hailing from the lead zirconate titanate (PZT) family, known for its elevated dielectric constant (He et al., 2023). Its remarkable piezoelectric coefficient and exceptional mechanical resilience (Fan et al., 1999) render it the material of paramount choice. To temper the overall elastic stiffness of the transducer, a polymer, such as epoxy, with a comparatively lower elastic modulus is utilized to separate the PZT rods.

Fig. 1b provides a frontal perspective of the simulation setup, showcasing the transducer's placement on the skin. Surrounding the skin is a perfectly matching layer (PML) strategically designed to efficiently absorb sound waves and faithfully emulate real biological skin tissue. The dashed line, precisely situated at the transducer's center and 0.1 mm beneath the skin's surface, serves as the measurement point for the peak AP.

In Fig. 1b, the piezoelectric active elements are strategically positioned between a backing layer (2 mm thick) and a matching layer (12 mm thick). The inclusion of the matching layer is instrumental in circumventing the impedance mismatch that often arises between the transducer and the target acoustic medium—in this case, the skin. The impedance mismatch, if unaddressed, can lead to the reflection of sound waves at the interface between the two media, resulting in both a loss of acoustic power (Zhao et al., 2022; Lee et al., 2022) at the desired location and distortions in the acoustic pattern. Various materials can be used for the matching layer, such as magnesium, polyurethane, polystyrene, and alumina (Al2O3). In our study, we chose alumina because its acoustic impedance is close to the geometric mean of the acoustic impedances of both the skin and PZT. For exact impedance values, see Table 1.

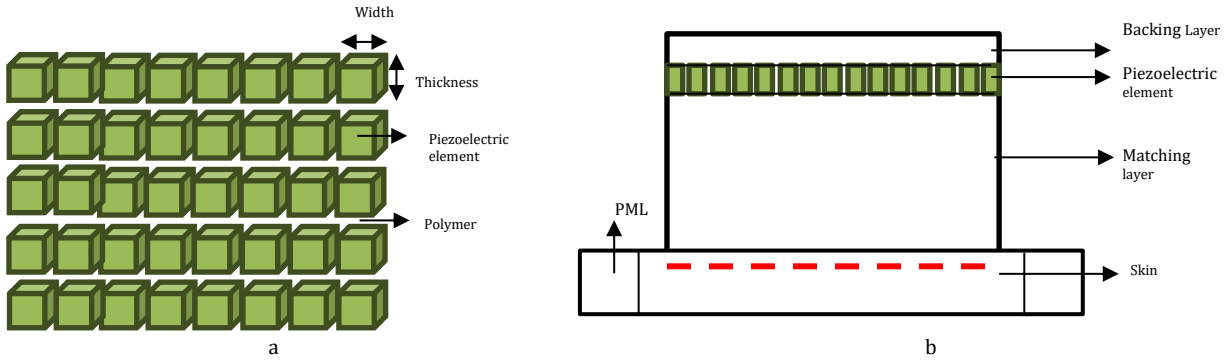

Fig. 1: (a) Piezoelectric 8 × 5 array elements (b) Front view of the simulation setup

Table 1: Primary materials used in the transducer

Parameter	Material	Speed of sound [m/s]	Density [kg/m^3]	Acoustic Impendence (Z) [MRayl]
PZT	PZT 4	4630	7500	34.4 (Castillo et al., 2003)
Epoxy	Epoxy resin	2554	1170	3 (Patricio Rodrigues et al., 2018)
Matching layer	Alumina	9900	3960	2.8 to 5.1 (Zhou et al., 2009)
Backing layer	Silver	3600	10490	0.529
Skin	Skin	1540	1020	1.5 (Wang et al., 2018)

It is important to note that the energy produced by the piezoelectric elements can travel in both forward and backward directions. To reduce unwanted backward radiation from the transducer, a 2 mm thick backing layer is placed at the back of the transducer. This backing layer effectively reduces the unwanted backward radiation, ensuring that most of the acoustic energy is directed toward the target area (Kim et al., 2022).

3. Simulation and results

We conducted comprehensive simulations of the sonophoretic PZT transducer using COMSOL Multiphysics, employing the Electrostatic (ES) and Solid Mechanics (SM) modules. Specifically, the modeling of the matching layer and backing layer was accomplished using the SM module, while the skin medium necessitated the Acoustic Pressure in the Frequency Domain (ACPR) module for assessing the AP induced by the transducer-generated sound waves.

The PZT transducers were systematically modeled in five distinct array sizes: 8×5, 10×6, 12×8, 14×9 and 16×10, all configured in a rectangular shape with consistent surface areas. Detailed parameters for the PZT elements and arrays are provided in Table 2. Each array maintained a uniform thickness of 3.2 mm, with a kerf width set at 1.5 mm, aligning with the thickness of commercially available dicing saws (as indicated in Table 2).

Table 2: Parameters used for array in the simulation

Parameters	Description	Values				
Array size	Number of elements in an array	8×5	10×6	12×8	14×9	16×10
Width (mm)	Width of piezoelectric element	2	1.5	1	0.75	0.5
Width-to-thickness ratio	Width to thickness ratio of each element	0.625	0.468	0.313	0.234	0.156
Area	Total area covered by transducer	$1.6 \times 2.65\ cm^2$				
Frequency	Number of cycles per second	20-40 kHz				
Kerf	The interval between consecutive elements	1.5 mm				

A uniform in-phase sinusoidal excitation with a peak voltage of 1 volt was applied to all elements within the arrays. Fig. 2 presents the results, showcasing the achieved APs across the five array sizes within the frequency range of 20-40 kHz. These peak APs were measured at a depth of 0.1 mm beneath the skin surface (indicated by the dashed red line in Fig. 1b). In Fig. 2, the solid line represents the minimum AP requirement for effective TDD, set at 0.23 MPa, while the dashed line signifies the maximum allowable MI, i.e., 1.9. The data points marked with symbols (◊, □, Δ, ×, ⁕, ○) correspond to the AP achieved with the 8×5, 10×6, 12×8, 14×9 and 16×10, array transducers, respectively.

Considering both the minimum required AP and the maximum allowable MI values, it is evident that the optimal frequency ranges for each array size are as follows: 29-33 kHz for 8×5, 28-32 kHz for 10×6, 27-30 kHz for 12×8, 26-29 kHz for 14×9 and 26-29 kHz for 16×10. Accordingly, we selected the mid-range frequency for each array size in our research.

We operated the five transducers at the mid-range frequencies identified in Fig. 2 and detailed in Table 3. Additionally, adhering to the principle of quarter-wave resonance (Ma et al., 2020), we opted for matching layer thicknesses equal to one-quarter of the wavelength (λ/4) to optimize results. Table 3 provides information on matching layer thicknesses, the number of elements, operating frequencies, and peak APs achieved by the array transducers.

An intriguing observation from Table 3 is that transducers with a greater number of elements yield higher peak APs. Consequently, we sought to establish a relationship between the number of PZT elements and peak AP within the 20-40 kHz frequency range, which appears to exhibit a linear trend.

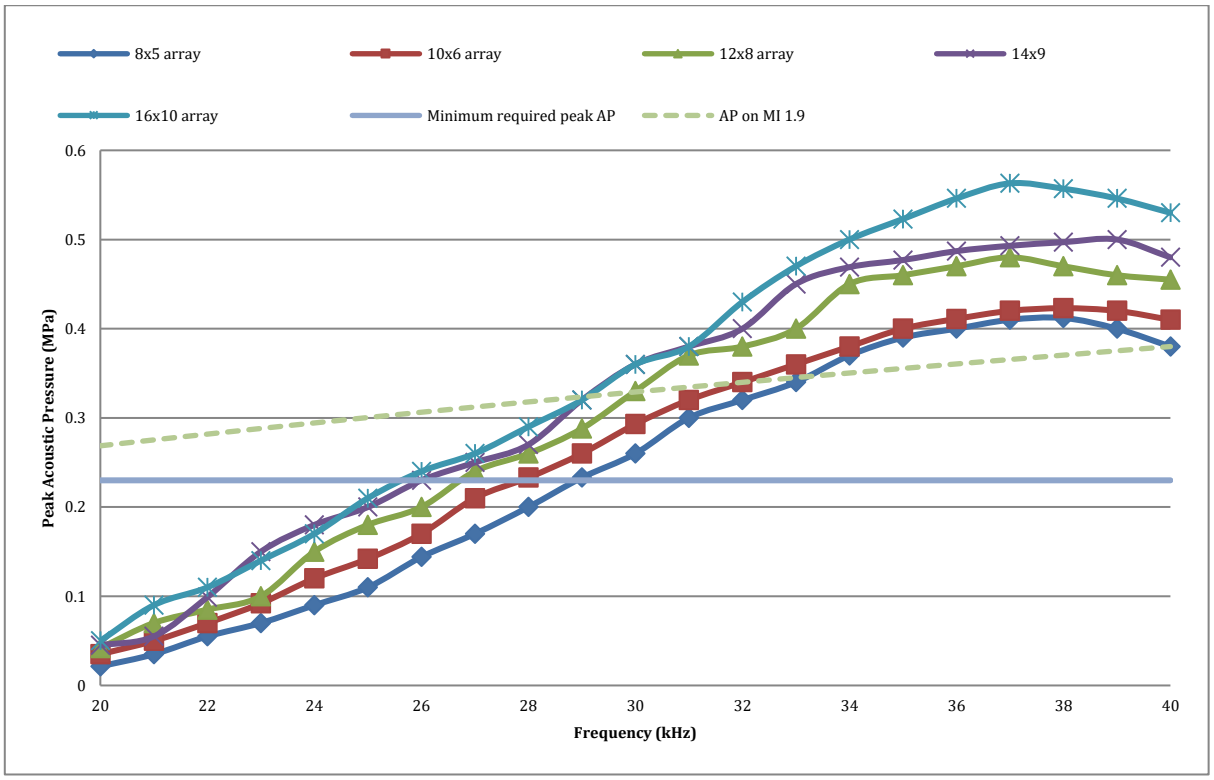

Fig. 2: Comparison of the AP of an array for fixed MI

Table 3: Peak AP of different arrays on 20-40 kHz

Transducer		Within MI limits			Regardless of MI	
Array size	Number of elements	Mid-range frequency (kHz)	AP (MPa)	Matching layer thickness ($\lambda/4$) mm	Frequency	Peak AP
8×5	40	31	0.32	14.7	38	0.38
10×6	60	30	0.32	15.2	38	0.41
12×8	96	28.5	0.33	15.8	37	0.455
14×9	126	27.5	0.35	16.1	39	0.495
16×10	160	27	0.36	16.5	37	0.537

Fig. 3 offers valuable insights into the distribution of AP fields at a plane situated 0.1 mm beneath the skin surface and parallel to it. Subfigures 3a and 3b depict the AP distributions achieved using the minimum array size of 8×5 and the maximum array size of 16×10, both selected for this research. Notably, these distributions reveal that AP is most concentrated at the center and diminishes radially outward. Furthermore, the pattern remains consistent despite variations in array size.

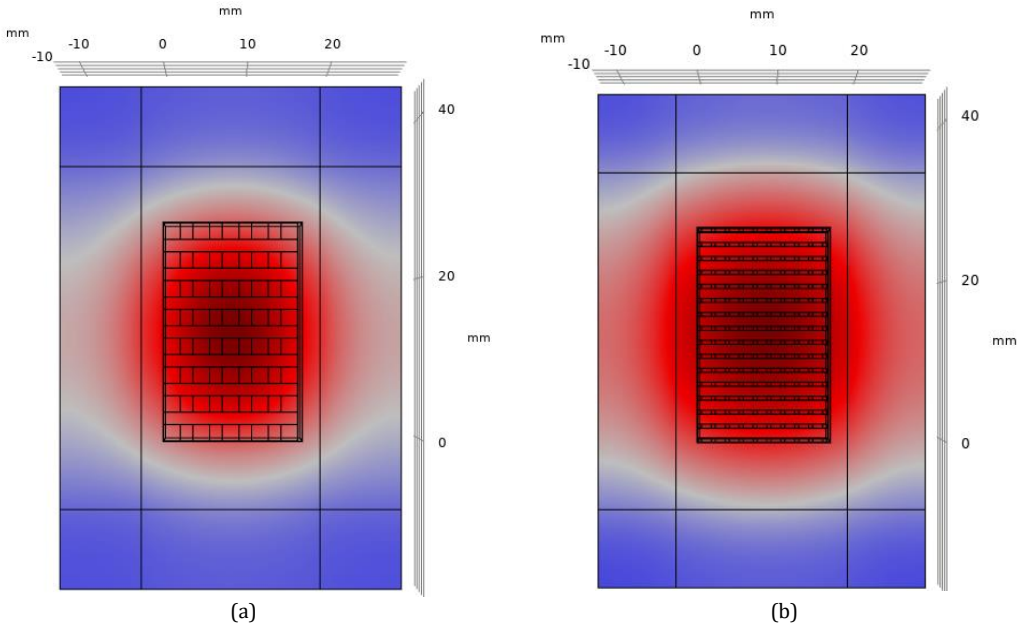

Fig. 3: Top-view of AP measured on the skin surface (a) 8×5 array (b) 16×10 array

4. Validation

To ensure the robustness and credibility of our simulation methodology and results, we conducted a validation exercise by simulating a previously published transducer design, yielding comparable outcomes to those reported (Kim and Jiang, 2023). The reference study, authored by Kim and Jiang (2023), involved the design and simulation of a miniaturized 1-3 piezoelectric composite ultrasound transducer using ANSYS. The transducer design encompassed various array sizes and operated at a frequency of 4 MHz with an applied voltage of 100 volts. We diligently replicated this design and conducted simulations using COMSOL, achieving results consistent with those documented in Table 4. Table 4 provides a comprehensive comparison of critical parameters. Columns 1 to 5 display the width of piezoelectric rods, the width-to-thickness ratio of rods, the array size, the recorded AP output in ANSYS, and the corresponding AP output in COMSOL, respectively. This validation step not only underscores the fidelity of our simulation approach but also demonstrates the reproducibility of results across different simulation platforms, bolstering the reliability of our findings.

Table 4: Validation of earlier simulation results

Width of piezoelectric rods (μm)	Dimension ratio (width-to-thick)	Size of array of rods	Max. AP (MPa)	Max. AP (MPa) COMSOL
200	0.625	8×8	2.97	2.81
100	0.313	16×16	6.65	6.36
50	0.156	32×32	7.60	7.49

5. Conclusion

The paper presents the design and simulation of five piezoelectric transducers, highlighting their ability to generate the necessary AP for TDD under specific voltage and frequency conditions. The study notably examines a range of array sizes 8×5, 10×6, 12×8, 14×9, and 16×10 and finding emphasizes the significant influence of array size on the performance of transducers while keeping the total area constant. The established link between array size and AP provides crucial guidance for enhancing TDD systems, indicating that larger arrays might be an effective strategy for improving the performance of transducers in TDD applications.

Additionally, the paper confirms the reliability of COMSOL simulations by comparing them with previous ANSYS simulations, showing highly consistent results. This comparison lends substantial validity to the simulation method used and the results obtained.

Future research will focus on using COMSOL simulations for specific TDD processes, like insulin delivery through a patch. Investigating the application of piezoelectric transducers for practical uses such as insulin delivery marks a significant step towards their real-world application. This work has the potential to revolutionize medical drug delivery, offering innovative and effective methods for enhancing patient care and health outcomes.

Compliance with ethical standards

Conflict of interest

The author(s) declared no potential conflicts of interest with respect to the research, authorship, and/or publication of this article.

References

Abe Y and Nishizawa M (2021). Electrical aspects of skin as a pathway to engineering skin devices. APL Bioengineering, 5(4): 041509. https://doi.org/10.1063/5.0064529 **PMid:34849444 PMCid:PMC8604566**

Ahmad A, Rasul T, Yousaf A, and Zaman U (2020). Understanding factors influencing elderly diabetic patients' continuance intention to use digital health wearables: Extending the technology acceptance model (TAM). Journal of Open Innovation: Technology, Market, and Complexity, 6(3): 81. https://doi.org/10.3390/joitmc6030081

Bruno BP, Fahmy AR, Stürmer M, Wallrabe U, and Wapler MC (2018). Properties of piezoceramic materials in high electric field actuator applications. Smart Materials and Structures, 28(1): 015029. https://doi.org/10.1088/1361-665X/aae8fb

Cai Y, Zhou Y, Zhang P, Kalia YN, Gratieri T, and Chen Y (2020). Tissue levels of flurbiprofen in the rat plantar heel after short-duration topical iontophoresis are sufficient to induce pharmacodynamic responses to local pain stimuli. Pharmaceutics, 12(7): 608. https://doi.org/10.3390/pharmaceutics12070608 **PMid:32629832 PMCid:PMC7408369**

Čáp I, Čápová K, Smetana M, and Borik Š (2021). Electromagnetic and acoustic waves in bioengineering applications. BoD–Books on Demand, Norderstedt, Germany. https://doi.org/10.5772/intechopen.101652

Castillo M, Acevedo P, and Moreno E (2003). KLM model for lossy piezoelectric transducers. Ultrasonics, 41(8): 671-679. https://doi.org/10.1016/S0041-624X(03)00101-X **PMid:14585479**

Conlon TW, Yousef N, Mayordomo-Colunga J, Tissot C, Fraga MV, Bhombal S, Suryawanshi P, Villanueva AM, Siassi B, and Singh Y (2022). Establishing a risk assessment framework for point-of-care ultrasound. European Journal of Pediatrics, 181(4): 1449–1457. https://doi.org/10.1007/s00431-021-04324-4 **PMid:34846557 PMCid:PMC8964607**

Cordery SF, Husbands SM, Bailey CP, Guy RH and Delgado-Charro MB (2019). Simultaneous transdermal delivery of buprenorphine hydrochloride and naltrexone hydrochloride by iontophoresis. Molecular Pharmaceutics, 16(6): 2808–2816. https://doi.org/10.1021/acs.molpharmaceut.9b00337 **PMid:31070927**

del Río-Sancho S, Pan Delgado D, de la Fuente GF, García-Caballero T, Taboada-Suárez A, Csaba N, Bao-Varela C, and José Alonso M (2020). Laser-induced transient skin disruption to enhance cutaneous drug delivery. European Journal of Pharmaceutics and Biopharmaceutics, 156: 165–175. https://doi.org/10.1016/j.ejpb.2020.08.027 **PMid:32891732**

Duncan B, Al-Kassas R, Zhang G, Hughes D, and Qiu Y (2023). Ultrasound-mediated ocular drug delivery: From physics and instrumentation to future directions. Micromachines, 14(8): 1575. https://doi.org/10.3390/mi14081575 **PMid:37630111 PMCid:PMC10456754**

Fan J, Stoll WA, and Lynch CS (1999). Nonlinear constitutive behavior of soft and hard PZT: Experiments and modeling. Acta Materialia, 47(17): 4415-4425. https://doi.org/10.1016/S1359-6454(99)00306-7

Fatahi Asl J, Farzanegan Z, Tahmasbi M, Birgani SM, Malekzade M, and Yazdaninejad H (2021). Evaluation of the scan duration and mechanical and thermal indices applied for the diagnostic ultrasound examinations. Journal of Ultrasound in Medicine, 40(9): 1839–1850. https://doi.org/10.1002/jum.15565 **PMid:33179801**

Geoghegan R, ter Haar G, Nightingale K, Marks L, and Natarajan S (2022). Methods of monitoring thermal ablation of soft tissue tumors – A comprehensive review. Medical Physics, 49(2): 769–791. https://doi.org/10.1002/mp.15439 **PMid:34965307**

Grey CP and Hall DS (2020). Prospects for lithium-ion batteries and beyond–A 2030 vision. Nature Communications, 11(1): 1-4. https://doi.org/10.1038/s41467-020-19991-4 **PMid:33293543 PMCid:PMC7722877**

Han X, Yi W, Chen S, Cai Z, Zhu Y, Han W, Guo X, Shen J, Cui W, and Bai D (2023). Ultrasound-responsive smart composite biomaterials in tissue repair. Nano Today, 49: 101804. https://doi.org/10.1016/j.nantod.2023.101804

He X, Lu Y, Chu T, Liao W, Li T, Liu X, Liang L, Li H, Dai X, Liu Y, and Zhou L (2023). High-stability quinary lead-based piezoelectric ceramics with high piezoelectric properties. Journal of Applied Physics, 134(14): 144103. https://doi.org/10.1063/5.0167214

Hsieh A, Baker MB, Phalen JM, Mejias-Garcia J, Hsieh A, Hsieh A, and Canelli R (2022). Handheld point-of-care ultrasound: Safety considerations for creating guidelines. Journal of Intensive Care Medicine, 37(9): 1146-1151. https://doi.org/10.1177/08850666221076041 **PMid:35118909 PMCid:PMC9393648**

Izadifar Z, Babyn P, and Chapman D (2017). Mechanical and biological effects of ultrasound: A review of present knowledge. Ultrasound in Medicine and Biology, 43(6): 1085–1104. https://doi.org/10.1016/j.ultrasmedbio.2017.01.023 **PMid:28342566**

Ji W, Liu L, Xing Z, Zhang D, Wang Y, Chen L, Chen Y, Sun X, and Du Y (2021). Total-focus ultrasonic imaging of defects in solids using a PZT piezoelectric micromachined ultrasonic transducer array. IEEE Transactions on Ultrasonics, Ferroelectrics, and Frequency Control, 68(4): 1380–1386. https://doi.org/10.1109/TUFFC.2020.3032988 **PMid:33090950**

Kim DM, Park SK, and Park SG (2021). A study on the performance evaluation criteria and methods of abdominal ultrasound devices based on international standards. Safety, 7(2): 31. https://doi.org/10.3390/safety7020031

Kim E, Erdos G, Huang S, Kenniston TW, Balmert SC, Carey CD, Raj VS, Epperly MW, Klimstra WB, Haagmans BL, Korkmaz E et al. (2020). Microneedle array delivered recombinant coronavirus vaccines: Immunogenicity and rapid translational development. EbioMedicine, 55: 102743. https://doi.org/10.1016/j.ebiom.2020.102743 **PMid:32249203 PMCid:PMC7128973**

Kim H and Jiang X (2023). Numerical study of a miniaturized, 1–3 piezoelectric composite focused ultrasound transducer. Applied Sciences, 13(1): 615. https://doi.org/10.3390/app13010615

Kim H, Yoo J, Heo D, Seo YS, Lim HG, and Kim HH (2022). High-attenuation backing layer for miniaturized ultrasound imaging transducer. IEEE Transactions on Ultrasonics, Ferroelectrics, and Frequency Control, 69(6): 1960–1969. https://doi.org/10.1109/TUFFC.2022.3164451 **PMid:35377844**

Kouritem SA, Al-Moghazy MA, Noori M, and Altabey WA (2022). Mass tuning technique for a broadband piezoelectric energy harvester array. Mechanical Systems and Signal Processing, 181: 109500. https://doi.org/10.1016/j.ymssp.2022.109500

Koznarska-Buczkowska A, Chilicka K, Rusztowicz M, and Adamczyk E (2022). The effectiveness of green tea and sonophoresis on oily skin: A case report. Medical Science Pulse, 16(1): 38–42. https://doi.org/10.5604/01.3001.0015.7911

Krisnamurti DGB, Purwaningsih EH, Antarianto RD, and Louisa M (2022). Glucose-responsive pectin insulin patch for diabetes mellitus: A review. In the 6th Biomedical Engineering's Recent Progress in Biomaterials, Drugs Development, And Medical Devices: Proceedings of the 6th International Symposium of Biomedical Engineering, AIP Publishing, Depok, Indonesia, 2537(1): 040014. https://doi.org/10.1063/5.0098287

Lee J and Rhee YS (2022). Ophthalmic dosage forms for drug delivery to posterior segment. Journal of Pharmaceutical Investigation, 52(2): 161-173. https://doi.org/10.1007/s40005-021-00554-8

Lee T, Jung J, Lee SM, Park J, Park JH, Paik KW, and Lee HJ (2022). FPCB as an acoustic matching layer for 1D linear ultrasound transducer arrays. Sensors, 22(15): 5557. https://doi.org/10.3390/s22155557 **PMid:35898059 PMCid:PMC9332256**

Li S, Xu J, Li R, Wang Y, Zhang M, Li J, Yin S, Liu G, Zhang L, Li B, Gu Q, and Su Y (2022). Stretchable electronic facial masks for sonophoresis. ACS Nano, 16(4): 5961–5974. https://doi.org/10.1021/acsnano.1c11181 **PMid:35363481**

Li Z, Guo R, Fei C, Li D, Chen D, Zheng C, Wu R, Feng W, and Yang Y (2021). Liquid lens with adjustable focus for ultrasonic imaging. Applied Acoustics, 175: 107787. https://doi.org/10.1016/j.apacoust.2020.107787

Liu HL and Hsieh CM (2009). Single-transducer dual-frequency ultrasound generation to enhance acoustic cavitation. Ultrasonics Sonochemistry, 16(3): 431–438. https://doi.org/10.1016/j.ultsonch.2008.08.009 **PMid:18951828**

Liu W, Zhu C, and Wu D (2021). Flexible piezoelectric micro ultrasonic transducer array integrated on various flexible substrates. Sensors and Actuators A: Physical, 317: 112476. https://doi.org/10.1016/j.sna.2020.112476

Lu T, Ji S, Jin W, Yang Q, Luo Q, and Ren TL (2023). Biocompatible and long-term monitoring strategies of wearable, ingestible and implantable biosensors: Reform the next generation healthcare. Sensors, 23(6): 2991. https://doi.org/10.3390/s23062991 **PMid:36991702 PMCid:PMC10054135**

Ma S, Liu C, Li B, Zhang T, Jiang L, and Wang R (2020). Sonophoresis enhanced transdermal delivery of cisplatin in the xenografted tumor model of cervical cancer. OncoTargets and Therapy, 13: 889–902. https://doi.org/10.2147/OTT.S238126 **PMid:32099393 PMCid:PMC6996214**

Martin K (2010). The acoustic safety of new ultrasound technologies. Ultrasound, 18(3): 110-118. https://doi.org/10.1258/ult.2010.010024

Mitra AK, Kwatra D, and Vadlapud AD (2014). Drug delivery. Jones and Bartlett Learning, Burlington, USA.

Moghaddam ZH, Mokhtari-Dizaji M, Movahedin M, and Ravari ME (2017). Estimation of the distribution of low-intensity ultrasound mechanical index as a parameter affecting the proliferation of spermatogonia stem cells in vitro. Ultrasonics

Sonochemistry, 37: 571–581.
https://doi.org/10.1016/j.ultsonch.2017.02.013
PMid:28427670

Moyano DB, Paraiso DA, and González-Lezcano RA (2022). Possible effects on health of ultrasound exposure, risk factors in the work environment and occupational safety review. Healthcare, 10(3): 423.
https://doi.org/10.3390/healthcare10030423
PMid:35326901 PMCid:PMC8954895

Nahavandi D, Alizadehsani R, Khosravi A, and Acharya UR (2022). Application of artificial intelligence in wearable devices: Opportunities and challenges. Computer Methods and Programs in Biomedicine, 213: 106541.
https://doi.org/10.1016/j.cmpb.2021.106541
PMid:34837860

Park J, Lee H, Lim GS, Kim N, Kim D, and Kim YC (2019). Enhanced transdermal drug delivery by sonophoresis and simultaneous application of sonophoresis and iontophoresis. AAPS PharmSciTech, 20: 96.
https://doi.org/10.1208/s12249-019-1309-z
PMid:30694397

Patricio Rodrigues E, Francisco de Oliveira T, and Buiochi F (2018). Development and characterization of a 2D phased array ultrasonic transducer for underwater applications. In the 24th ABCM International Congress of Mechanical Engineering, Rio de Janeiro, Brazil.
https://doi.org/10.26678/ABCM.COBEM2017.COB17-2391

Peng H, Qian X, Mao L, Jiang L, Sun Y, and Zhou Q (2019). Ultrafast ultrasound imaging in acoustic microbubble trapping. Applied Physics Letters, 115(20): 203701.
https://doi.org/10.1063/1.5124437

Phatale V, Vaiphei KK, Jha S, Patil D, Agrawal M, and Alexander A (2022). Overcoming skin barriers through advanced transdermal drug delivery approaches. Journal of Controlled Release, 351: 361–380.
https://doi.org/10.1016/j.jconrel.2022.09.025
PMid:36169040

Quarato CMI, Lacedonia D, Salvemini M, Tuccari G, Mastrodonato G, Villani R, and Sperandeo M (2023). A review on biological effects of ultrasounds: Key messages for clinicians. Diagnostics, 13(5): 855.
https://doi.org/10.3390/diagnostics13050855
PMid:36899998 PMCid:PMC10001275

Sá GFF, Serpa C, and Arnaut LG (2013). Stratum corneum permeabilization with photoacoustic waves generated by piezophotonic materials. Journal of Controlled Release, 167(3): 290–300.
https://doi.org/10.1016/j.jconrel.2013.02.005
PMid:23419949

Seah BCQ and Teo BM (2018). Recent advances in ultrasound-based transdermal drug delivery. International Journal of Nanomedicine, 13: 7749.
https://doi.org/10.2147/IJN.S174759
PMid:30538456 PMCid:PMC6251463

Sekhar MC, Veena E, Kumar NS, Naidu KCB, Mallikarjuna A, and Basha DB (2023). A review on piezoelectric materials and their applications. Crystal Research and Technology, 58(2): 2200130. https://doi.org/10.1002/crat.202200130

Şen T, Tüfekçioğlu O, and Koza Y (2015). Mechanical index. Anatolian Journal of Cardiology, 15(4): 334-336.
https://doi.org/10.5152/akd.2015.6061
PMid:25880292 PMCid:PMC5336845

Seneviratne S, Hu Y, Nguyen T, Lan G, Khalifa S, Thilakarathna K, Hassan M, and Seneviratne A (2017). A survey of wearable devices and challenges. IEEE Communications Surveys and Tutorials, 19(4): 2573–2620.
https://doi.org/10.1109/COMST.2017.2731979

Singh P, Muhammad IJ, Nelson NE, Tran KT, Vinikoor T, Chorsi MT, and Nguyen TD (2022). Transdermal delivery for gene therapy. Drug Delivery and Translational Research, 12(11): 2613-2633.
https://doi.org/10.1007/s13346-022-01138-1
PMid:35538189 PMCid:PMC9089295

Tu L, Liao Z, Luo Z, Wu YL, Herrmann A, and Huo S (2021). Ultrasound-controlled drug release and drug activation for cancer therapy. Exploration, 1(3): 20210023.
https://doi.org/10.1002/EXP.20210023
PMid:37323693 PMCid:PMC10190934

Vaidya J and Shende P (2020). Potential of sonophoresis as a skin penetration technique in the treatment of rheumatoid arthritis with transdermal patch. AAPS PharmSciTech, 21(5): 1-9.
https://doi.org/10.1208/s12249-020-01725-w
PMid:32601758

Wang B, Long Z, Hong Y, Pan Q, Lin W, and Yang Z (2021). Woodpecker-mimic two-layer band energy harvester with a piezoelectric array for powering wrist-worn wearables. Nano Energy, 89: 106385.
https://doi.org/10.1016/j.nanoen.2021.106385

Wang Y, Tao J, Guo F, Li S, Huang X, Dong J, and Cao W (2018). Magnesium alloy matching layer for high-performance transducer applications. Sensors, 18(12): 4424.
https://doi.org/10.3390/s18124424
PMid:30558141 PMCid:PMC6308683

Yu CC, Shah A, Amiri N, Marcus C, Nayeem MOG, Bhayadia AK, Karami A, and Dagdeviren C (2023). A conformable ultrasound patch for cavitation-enhanced transdermal cosmeceutical delivery. Advanced Materials, 35(23): 2300066.
https://doi.org/10.1002/adma.202300066 **PMid:36934314**

Yu YQ, Yang X, Wu XF, and Fan YB (2021). Enhancing permeation of drug molecules across the skin via delivery in nanocarriers: novel strategies for effective transdermal applications. Frontiers in Bioengineering and Biotechnology, 9: 646554.
https://doi.org/10.3389/fbioe.2021.646554
PMid:33855015 PMCid:PMC8039394

Zaid Alkilani A, McCrudden MT, and Donnelly RF (2015). Transdermal drug delivery: Innovative pharmaceutical developments based on disruption of the barrier properties of the stratum corneum. Pharmaceutics, 7(4): 438-470.
https://doi.org/10.3390/pharmaceutics7040438
PMid:26506371 PMCid:PMC4695828

Zhang Z, Xu J, Yang L, Liu S, Xiao J, Li X, Wang X, and Luo H (2018). Design and comparison of PMN-PT single crystals and PZT ceramics based medical phased array ultrasonic transducer. Sensors and Actuators A: Physical, 283: 273–281.
https://doi.org/10.1016/j.sna.2018.09.067

Zhao J, Li Z, Fei C, Hou C, Wang D, Lou L, Chen D, Li D, Chen Z, and Yang Y (2022). Ultrawide bandwidth high-frequency ultrasonic transducers with gradient acoustic impedance matching layer for biomedical imaging. IEEE Transactions on Ultrasonics, Ferroelectrics, and Frequency Control, 69(6): 1952–1959.
https://doi.org/10.1109/TUFFC.2022.3141203
PMid:35020592

Zhou Q, Cha JH, Huang Y, Zhang R, Cao W, and Shung KK (2009). Alumina/epoxy nanocomposite matching layers for high-frequency ultrasound transducer application. IEEE Transactions on Ultrasonics, Ferroelectrics, and Frequency Control, 56(1): 213–219.
https://doi.org/10.1109/TUFFC.2009.1021
PMid:19213648 PMCid:PMC2729565

Zhu P, Peng H, Mao L, and Tian J (2021). Piezoelectric single crystal ultrasonic transducer for endoscopic drug release in gastric mucosa. IEEE Transactions on Ultrasonics, Ferroelectrics, and Frequency Control, 68(4): 952–960.
https://doi.org/10.1109/TUFFC.2020.3026320
PMid:32970594